Electronic Supplementary Information

Quantifying defect-enhanced chemical functionalization of single-layer graphene and its application in supramolecular assembly

Xiao-Liang Ye[1], Jun Cai[1], Xiao-Dong Yang[1], Xing-Yan Tang[1], Zhi-You Zhou[1], Yuan-Zhi Tan[1], Su-Yuan Xie[1], Lan-Sun Zheng[1]

[1] Collaborative Innovation Center of Chemistry for Energy Materials, State Key Laboratory for Physical Chemistry of Solid Surfaces, and Department of Chemistry, College of Chemistry and Chemical Engineering, Xiamen University, Xiamen 361005, China
*Correspondence to: yuanzhi_tan@xmu.edu.cn

Methods and Discussion

S1 Pristine graphene sample

Single-layer graphene (SLG) was grown on 25 μm thick Cu foil (Alfa Aesar, item No. 13382) using the typical chemical vapor deposition (CVD) method. After growth, an anisole solution of polymethyl methacrylate (PMMA, MW=950 K) was spin-coated on the top side of the graphene/Cu foil at 3000 rpm for 40 s. Then the PMMA film was kept at room temperature for 2 h. Graphene normally grows on the both sides of Cu foil. For transferring SLG, graphene at the back side was removed by oxygen plasma. Then, the Cu substrate was etched in an ammonium persulfate aqueous solution overnight. The PMMA/graphene film was transferred to a 300 nm SiO_2/Si substrate and then annealed at 180 ℃ for 15 min in a drying oven. After that, the PMMA layer was removed by acetone vapor and the pristine SLG on 300 nm SiO_2/Si substrate was obtained and designated as G0A (Fig. 1a). The quality of G0A was checked by Raman spectroscopy and optmicroscopy (Fig. 2a-2c and S1).

S2 Defect manipulation

To fabricate the defective SLGs, a layer of PMMA (MW=950 K) was spin-coated on the top of G0A (2000 rpm, 30 s). The Ar$^+$ plasma bombardment was employed to introduce defect and the defect density was controlled by variation of exposure time. The Ar$^+$ plasma treatment was carried out at a pressure of 100 Pa and a power of 6.8 W, using inductively coupled plasma at a radio frequency of 13.56 MHz (Middle Level). The low power of Ar$^+$ plasma can avoid rapid damage of SLG. The defective SLGs with different defect density (n_d) were obtained by irradiating for 12.0, 12.5, 13.0, and 14.0 min, which were labelled as G0B, G0C, G0D and G0E, respectively (Fig. 1b). The PMMA layer on G0B, G0C, G0D and G0E was removed by the acetone vapor before further functionalization.

S3 Raman analysis

Raman spectra were acquired with 532 nm and 638 nm laser excitation (638 nm for G2 samples to characterize the grafted FePc). Raman spectra mapping was carried out on Xplora (Horiba Jobin Ynon, France) in a fast line scanning mode with a 50× objective. To gain better spectral resolution, Raman spectrum of single spot was acquired by Xplora with 1200 lines mm^{-1} grating. The laser power was kept at 1 mW for G0 and G1 samples and 0.1 mW for G2 samples, with a typical acquisition time of 5 s. For each sample, eight Raman spectra from different spots were acquired and averaged. All the Raman spectra shown were normalized with the intensity of G band.

S4 Calculation of n_d for G0A-G0E

A quantitative formula has been proposed to correlate the mean distance between defects (L_d) with the intensity ratio of I_D/I_G (equation S1)[1] and n_d (cm^{-2}) is given by $n_d = 10^{14}/\pi L_d^2$.[2] Accordingly, n_d of G0A-G0E was calculated based on their I_D/I_G ratio and listed in Table S1.

$$\frac{I_D}{I_G} = C_A \frac{r_a^2 - r_d^2}{r_a^2 - 2r_d^2}[e^{-\pi r_d^2/L_d^2} - e^{-\pi(r_a^2 - r_d^2)/L_d^2}] \quad \text{(equation S1)}$$

S5 Synthesis of pyridinyl grafted SLGs (G1A$_1$-G1E$_1$)

The pyridinyl functionalization of SLGs was carried out in the same tube to avoid the variation in reaction conditions and the SLGs with different n_d on SiO$_2$/Si substrate were used directly without transfer.[3] Briefly, 0.4706 g of 4-aminopyridine (4-AP) was dissolved in 4 mL 6 mol L^{-1} HCl and cooled to 0 ℃ by ice bath. Then 0.3450 g of NaNO$_2$ was dissolved in 6 mL H$_2$O, cooled to 0 ℃ and added dropwise to the solution of 4-AP. The resulting yellow solution was maintained at 0 ℃ in ice bath, stirred for 30 min and added dropwise to the solution of sodium dodecyl sulfate (SDS) (0.50 g of SDS in 90 mL H$_2$O) at 0 ℃. After 5 min stirring, five pieces of SLGs with different n_d were immersed into the solution for 6 h at 0 ℃ to prepare the pyridinyl grafted SLGs, which are designated as G1A$_1$-G1E$_1$, respectively. After functionalization, G1A$_1$-G1E$_1$ were rinsed with isopropanol (IPA) and ultra-pure water to remove any adsorbed molecules (Fig. 1c and S2). Three parallel batches of G1A$_1$-G1E$_1$ series were prepared for further X-ray photoelectron spectroscopy (XPS) analysis.

S6 Synthesis of acridinyl grafted SLGs (G1A$_2$-G1E$_2$)

The acridinyl grafting of SLGs was carried out in the same tube to avoid the variation in reaction conditions as well and the defective SLGs with different n_d on the SiO$_2$/Si substrate were used directly without transfer. For acridinyl grafted SLGs, 9-aminoacridine (9-AA) (100 mg) was dissolved in 14 mL 6 mol L^{-1} HCl and cooled to 0 ℃ by ice bath. 0.3450 g of NaNO$_2$ was dissolved in 6 mL H$_2$O, cooled to 0 ℃, added dropwise to the solution of 9-AA and then stirred for 30 min at 0 ℃. The resulting solution was added dropwise into the solution of SDS (0.50 g of SDS in 80 mL H$_2$O, 0 ℃). After stirring for 5 min, five pieces of defective SLGs with different n_d were immersed for 6 h at 0 ℃ to prepare the acridinyl grafted SLGs, which were designated as G1A$_2$-G1E$_2$, respectively. After functionalization, G1A$_2$-G1E$_2$ were rinsed with IPA and ultra-pure water to remove any adsorbed molecules (Fig. 1e and S3). Generally, three parallel batches of G1A$_2$-G1E$_2$ series were produced for further XPS analysis

S7 Synthesis of 4-nitrobenzenyl grafted SLGs (G1A$_3$-G1E$_3$)

The 4-nitrobenzenyl grafting of SLGs were also carried out in the same tube to avoid the variation in reaction conditions and the SLGs with different n_d on the SiO$_2$/Si substrate were used directly without transfer. For 4-nitrobenzenyl grafted SLGs, 2 mmol of 4-nitrobenzenediazonium tetrafluoroborate and 0.50 g of SDS were dissolved in 100 mL H$_2$O. Then five pieces of SLGs with different n_d were immersed in the solution for 6 h at 0 ℃. After reaction, the 4-nitrobenzenyl grafted SLGs, which were designated as G1A$_3$-G1E$_3$, were obtained after rinsed carefully with IPA and ultra-pure water and stored for further experiments (Fig. 1f and S4). Generally, three parallel batches of G1A$_3$-G1E$_3$ series were produced for further XPS analysis.

S8 XPS analysis

XPS measurements were carried out on PHI quantum-2000 (Monochromatic Al K$_\alpha$ with ure1486.6 eV operating at 15 kV and 300 W). The base pressure of the system was 5.0×10^{-8} Pa.

First, the XPS of G0A was measured. In Fig. S5, high resolution XPS of G0A shows a symmetrical peak of C 1s at 284.7 eV, corresponding to the sp^2 carbon of graphene and no signal of nitrogen was found. The XPS measurement confirmed the high quality of G0A without nitrogen doping.

S9 XPS spectra of G1A$_1$-G1E$_1$

In the C 1s spectra of G1A$_1$-G1E$_1$ (Fig. S6), the covalent functionalization with pyridinyl was obviously evidenced by the peak at 286.1 eV for sp^3 hybridized carbon, which was not observed for G0A (Fig. S5). In the N 1s spectra (Fig. S6), the peak at 400.2 eV raised, indicating the grafting of pyridinyl groups. The N 1s at.% of G1A$_1$ to G1E$_1$ ranged from 1.20 % to 4.65 % (Table S2).

S10 XPS spectra of G1A$_2$-G1E$_2$

When acridinyl groups were grafted on G1A$_2$-G1E$_2$, beside the peak located at 286.1 eV for sp^3 hybridized carbon, two

deconvoluted peaks at 400.4 eV and 402.8 eV raised (Fig. S7), corresponding to the nitrogen atom of acridinyl group.

Peak at 406.9 eV was due to the slightly oxidation of acridinyl groups on G1A$_2$-G1E$_2$. The N 1s at.% of G1A$_2$ to G1E$_2$

ranged from 1.35 % to 3.25 % (Table S3).

S11 XPS spectra of G1A$_3$-G1E$_3$

When 4-nitrobenzenyl groups were grafted on G1A$_3$-G1E$_3$, beside the peak located at 286.1 eV for sp^3 hybridized

carbon, two well-fined peaks at 400.4 eV and 406.2 eV raised (Fig. S8), indicating the nitrogen atom of nitrophenyl. The

peak at the lower binding energy (400.4 eV) of N 1s is ascribed to the partial reduction of the nitro, due to the irradiation

during the XPS measurements.[4] The N 1s at.% of G1A$_3$ to G1E$_3$ ranged from 5.76 % to 8.68 % (Table S4).

S12 Defect type of defective SLGs

The defect type of SLGs is sensitive to the $I_D/I_{D'}$ ratio.[5] The I_D/I_G and $I_{D'}/I_G$ of a series of defective SLGs fabricated by

our Ar$^+$ plasma bombardment was plotted in Fig. S9 and by linear fitting the average $I_D/I_{D'}$ ratio was found to be 6.73,

close to the typical $I_D/I_{D'}$ ratio (7) of vacancy defects.

S13 Definition of degree of functionalization (F_{SLG})

F_{SLG} is defined by the ratio of the number of grafted groups to that of carbon atoms of graphene (see equation S2

below). Alternatively, it can be expressed as the ratio of the nitrogen content (N 1s at.%) to the carbon content of

graphene (C$_g$ at.%).

$$F_{\text{SLG}} = \frac{N_{\text{FG}}}{N_{\text{g}}} = \frac{\text{N 1s at.\%}}{\text{C}_{\text{g}} \text{ at.\%}} = \frac{\text{N 1s at.\%}}{\text{C}_{\text{Tot.}} \text{ at.\%} - \text{C}_{\text{FG}} \text{ at.\%}}$$ (equation S2)

Where N_{FG} and N_{g} represent the numbers of aryl functionalities and of carbons of graphene, respectively. The total carbon

content ($\text{C}_{\text{Tot.}}$ at.%) is the sum of the carbon contents in both graphene itself (C_{g} at.%) and in the grafted aryl groups (C_{FG}

at.%). Therefore, the F_{SLG} of each functionalized SLG (G1A$_1$-G1E$_1$, G1A$_2$-G1E$_2$ and G1A$_3$-G1E$_3$) can be measured by

XPS experimentally (Table S2-S4).

S14 Synthesis of G2A$_1$-G2E$_1$ by supramolecular assembly

To produce G2A$_1$-G2E$_1$, G1A$_1$-G1E$_1$ were immersed into the tetrahydrofuran (THF) solution of iron phthalocyanine

(FePc, 5 mg L^{-1}) at 60 ℃ for 6 h (Fig. 1d and S10) in the same tube. After carefully rinsed with THF, IPA, and H$_2$O

sequentially, G2A$_1$-G2E$_1$ were stored in dark for further characterization. For comparison, SLG with physically absorbed

FePc (FePc@Gr) was prepared by immersing G0A into the THF solution of FePc directly under similar conditions.

S15 XPS analysis of G2A$_1$-G2E$_1$

Fig. S12 displayed the XPS of G2A$_1$ to G2E$_1$ for Fe 2p respectively. The Fe 2p spectra were deconvoluted into two

well-defined peaks at 710.6 eV and 723.6 eV, corresponding to Fe 2p3/2 and Fe 2p1/2, respectively.

S16 Electrochemical catalysis measurement

SLGs appended with FePc-pyridinyl complex on SiO$_2$/Si substrate (G2A$_1$-G2E$_1$) were fabricated into working

electrode directly without transfer and their ORR catalytic activity was evaluated using these fabricated electrodes as

working electrode. Briefly, a copper wire was stuck to the graphene plane of SLGs by conductive silver paint to contact

with an external circuit. The electrical contact and the edge of graphene was then covered with epoxy and the area of

exposed graphene plane on the working electrode was measured by a ruler.[6] The ORR catalytic performance was

measured in O_2-saturated 0.1 M H_2SO_4 at 30 ℃ by a CHI-760D bipotentiostat. A GC plate and a reversible hydrogen

electrode (RHE) were used as counter electrode and reference electrode. The scan rate for all measurements was at 10

mV s^{-1} from 1.0 to 0.2 V. Ohmic drop of solution was compensated. Capacitive background current was corrected by

subtracting the curve recorded in N_2-saturated solution. Similarly, FePc@Gr, G0A-G0E, and $G1A_1$-$G1E_1$ (Fig. S17-S19)

were fabricated into working electrode and their ORR activity was investigated under the same conditions, which was

shown in Fig. S17-S19.

S17 Spatial patterning of functionalization for SLG

A layer of PMMA (MW=950 K) was spin-coated on the top of G0A (Fig. S20a). Then the sample was covered by a

metal mask patterned with U character (Fig. S20b) and was exposed to Ar^+ plasma to introduce defect at the exposed area

artificially (Fig. S20b), while the rest "covered region" remained intact (Fig. S20c). After that, the SLG with patterned

defective area was then grafted with pyridinyl group (Fig. S20d) and sequentially coordinated with FePc (Fig. S20e) as

described above. The obtained sample was used for further Raman analysis.
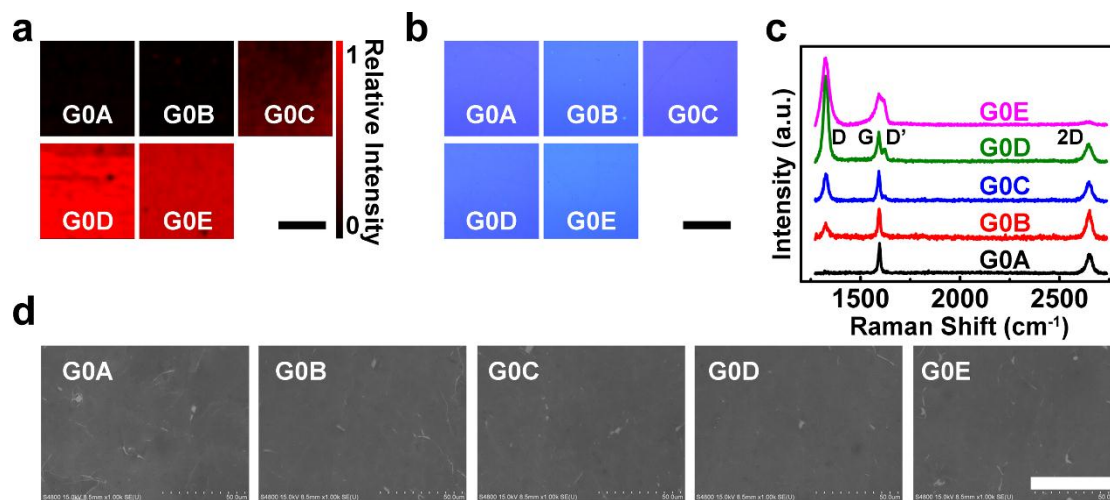
Fig. S1 (a) Raman mapping of the D bands and (b) optical images of SLGs.

(c) Typical Raman spectra of G0A-G0E (Raman spectra were acquired with 638 nm laser excitation).

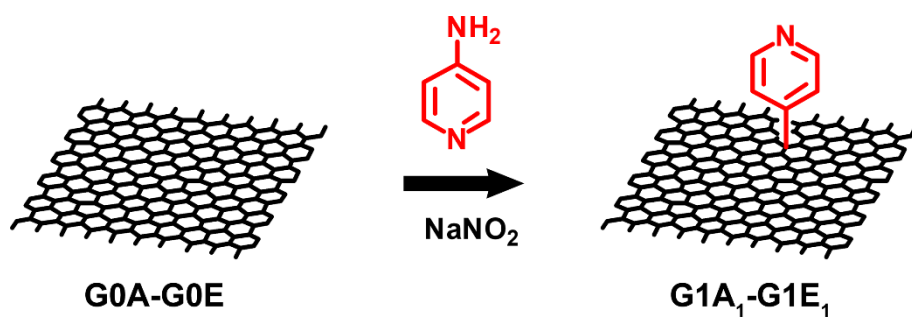(d) SEM images of G0A-G0E. The scale bars in (a), (b), and (d) indicate a distance of 50 μm.

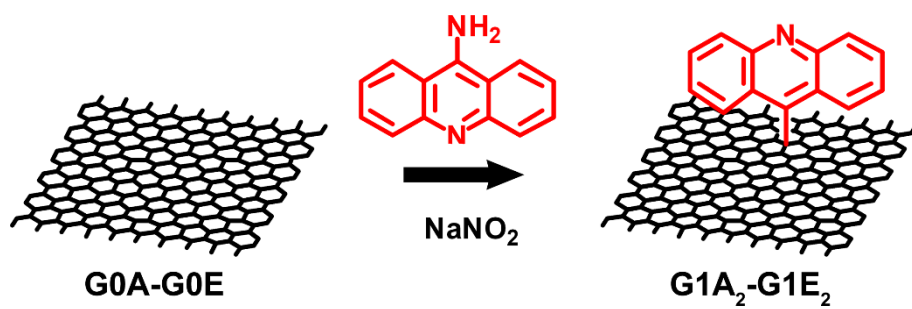**Fig. S2** Schematic diagram for pyridinyl functionalization to synthesize $G1A_1$-$G1E_1$.

G0A-G0E $\xrightarrow{\text{NaNO}_2}$ **G1A$_2$-G1E$_2$**

Fig. S3 Schematic diagram of acridinyl functionalization to synthesize G1A$_2$-G1E$_2$.
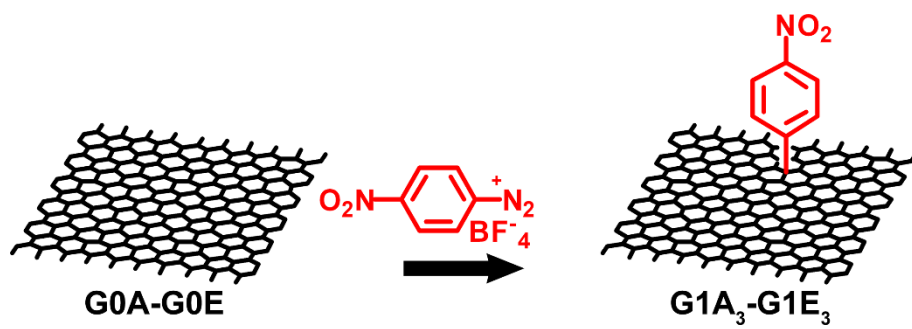
Fig. S4 Schematic diagram of 4-nitrobenzenyl functionalization to synthesize $G1A_3$-$G1E_3$.
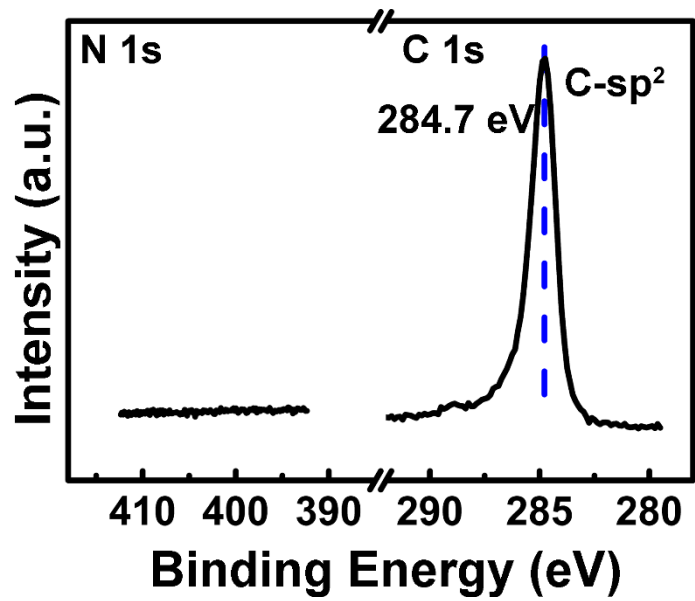
Fig. S5 XPS spectra of G0A.
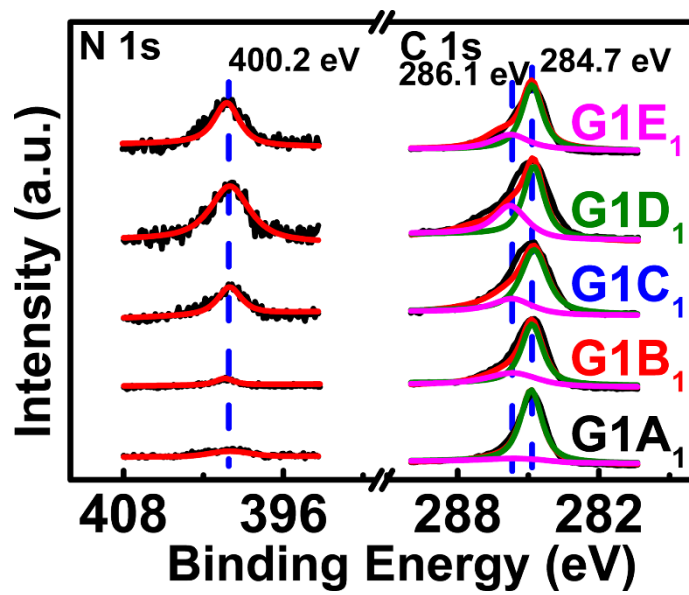
Fig. S6 XPS of C 1s and N 1s of G1A$_1$ to G1E$_1$.
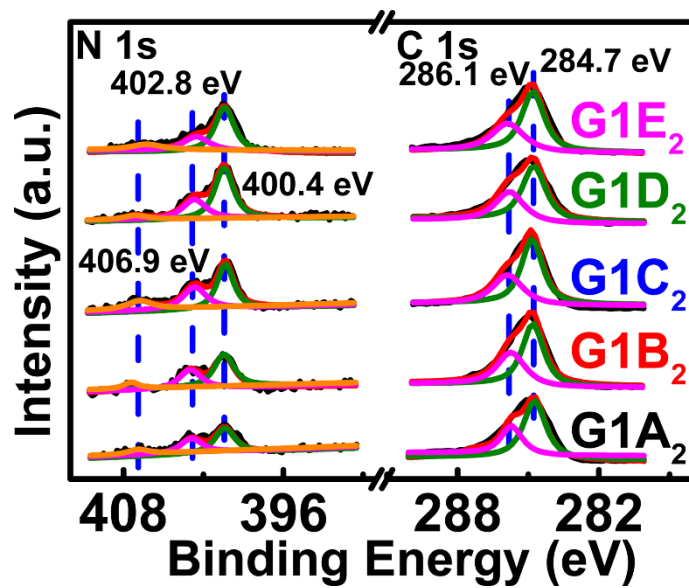
Fig. S7 XPS of C 1s and N 1s of G1A$_2$ to G1E$_2$.
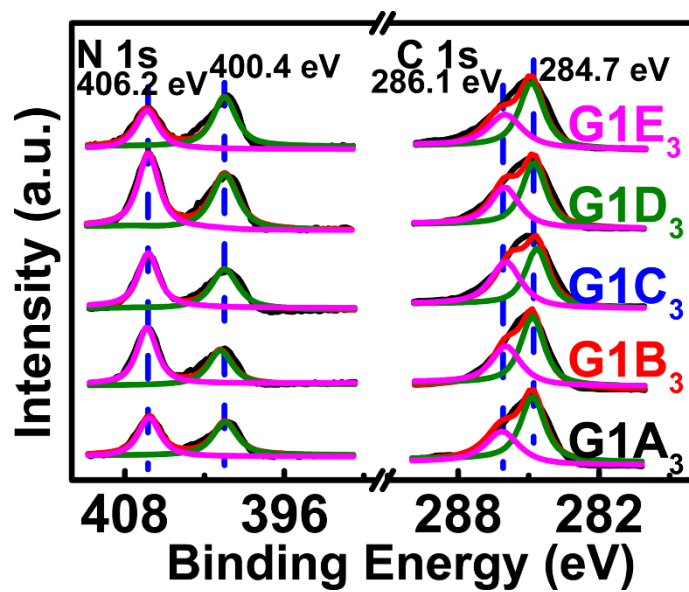
Fig. S8 XPS of C 1s and N 1s of G1A$_3$ to G1E$_3$.
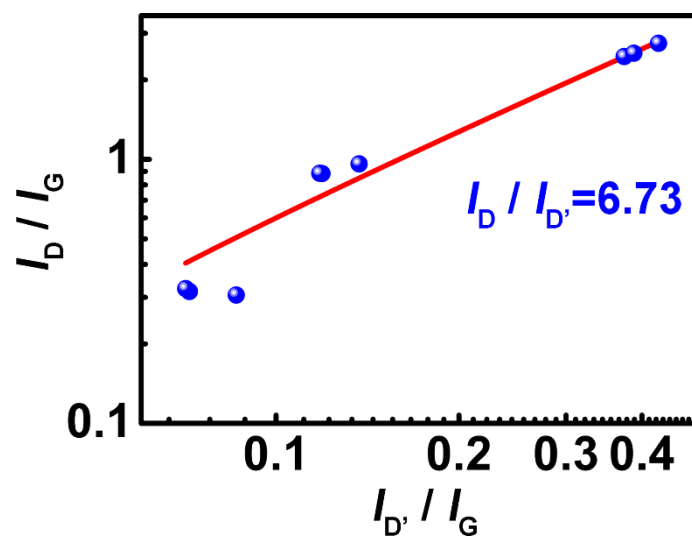
Fig. S9 The plot of I_D/I_G versus $I_{D'}/I_G$. Data were obtained from the Raman spectra of G0B, G0C and G0D used for
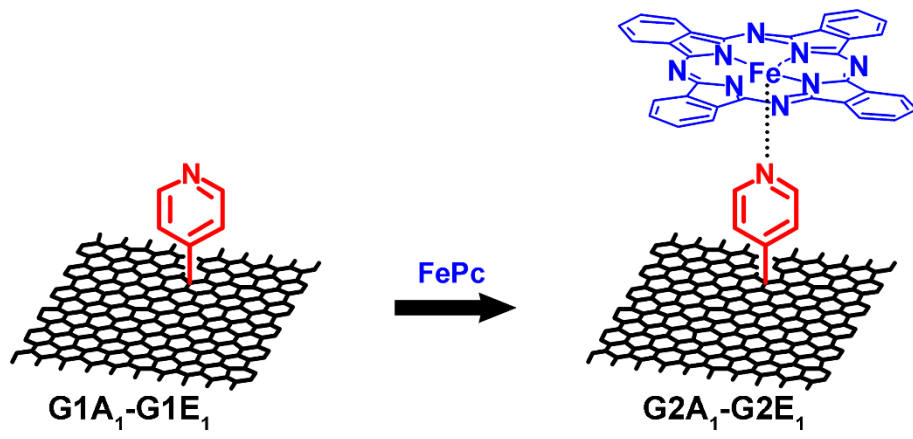
further chemical functionalization.

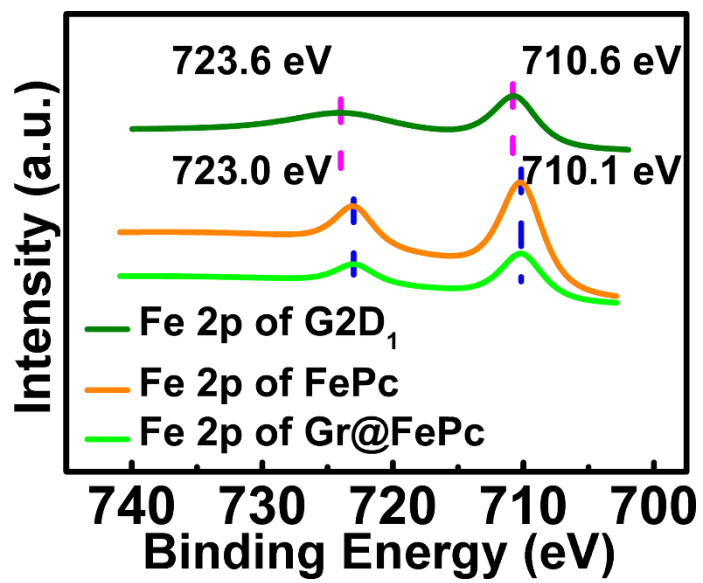**Fig. S10** Schematic diagram for the preparation of G2A$_1$-G2E$_1$.

Fig. S11 XPS of Fe 2p for G2D$_1$, FePc, and Gr@FePc.
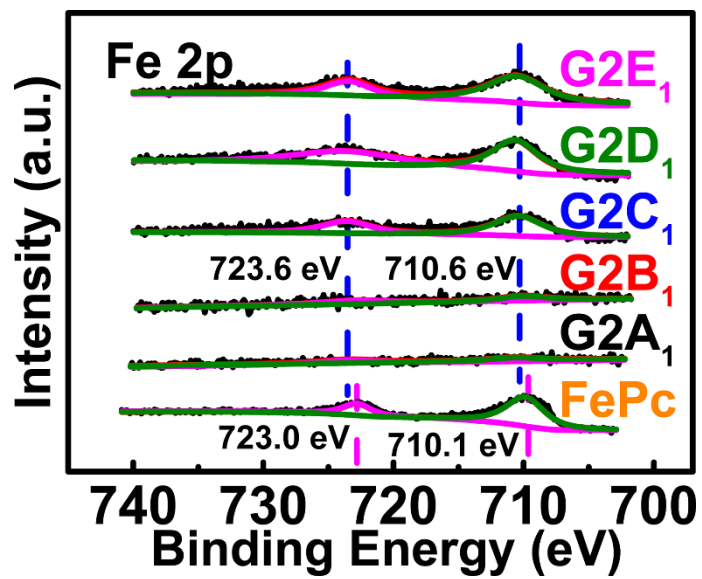
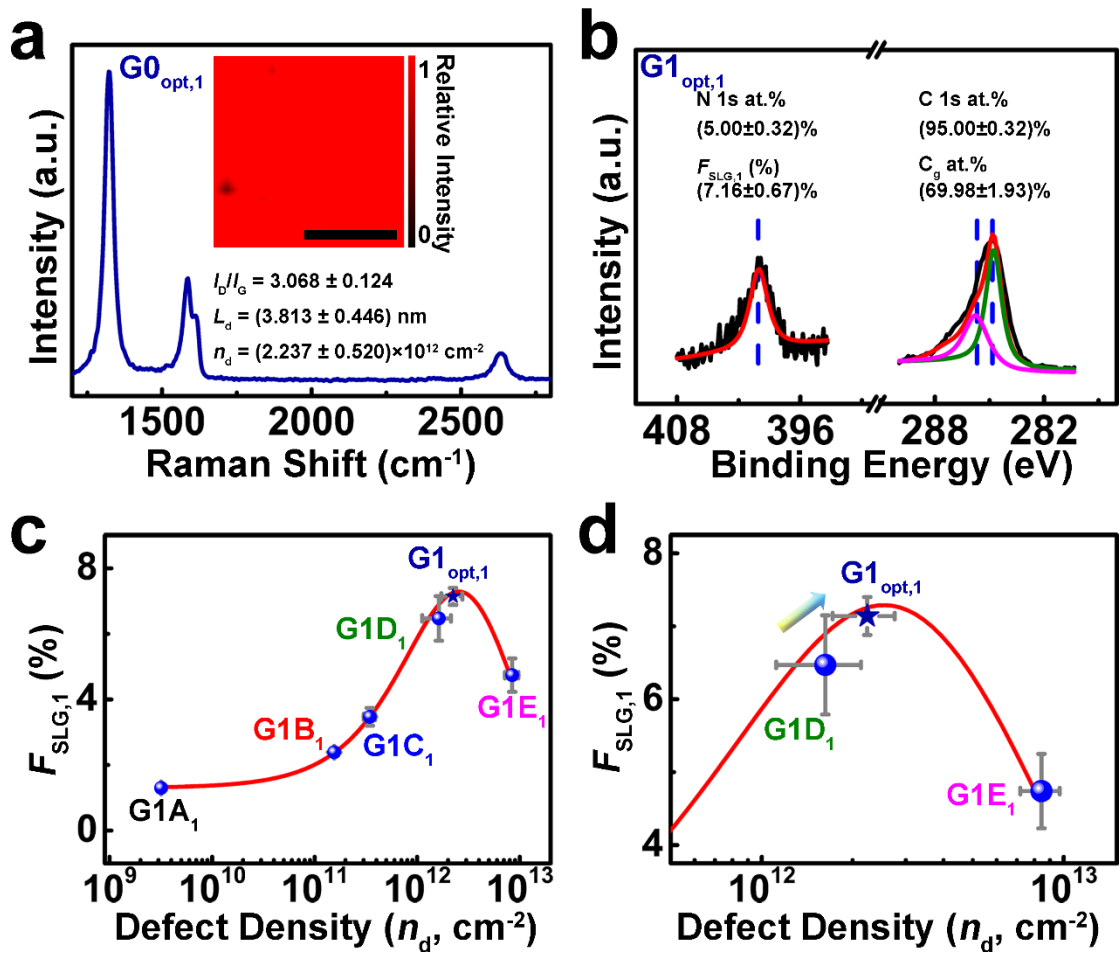**Fig. S12** XPS of Fe 2p for G2A$_1$-G2E$_1$ and pure FePc.

Fig. S13 (a) Typical Raman spectra of $G0_{opt,1}$. Inset: Raman mapping of the D band of $G0_{opt,1}$ (The scale bars indicate a distance of 50 μm.). (b) High resolution XPS of C 1s and N 1s in $G1_{opt,1}$. (c) The mathematic relationship between $F_{SLG,1}$ of G1 samples and n_d, magnified in (d). Solid lines are fit curves according to equation 3. The $G1_{opt,1}$ sample with optimized $F_{SLG,1}$ was plotted as pentacle in dark blue. With the higher and optmized n_d of $G1_{opt,1}$ than $G1D_1$, more functionalization degree $F_{SLG,1}$ achieved in $G1_{opt,1}$.
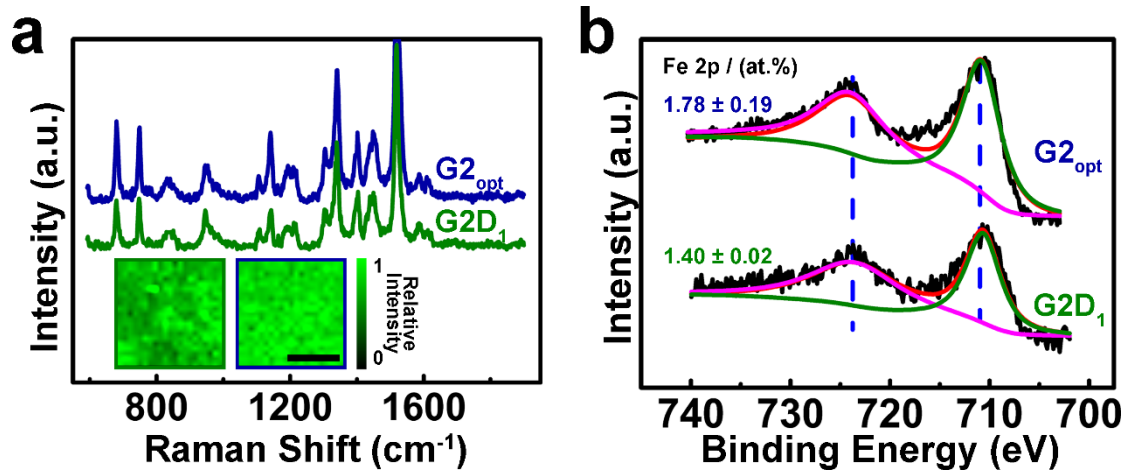
Fig. S14 The Raman spectra of $G2D_1$ and $G2_{opt}$. Inset: The Raman mappings of $G2D_1$ and $G2_{opt}$ using the spectral

regions mentioned in Fig. 4, Scale bar in (a) indicates a distance of 50 μm. (b) XPS of Fe 2p for $G2D_1$ and $G2_{opt}$.
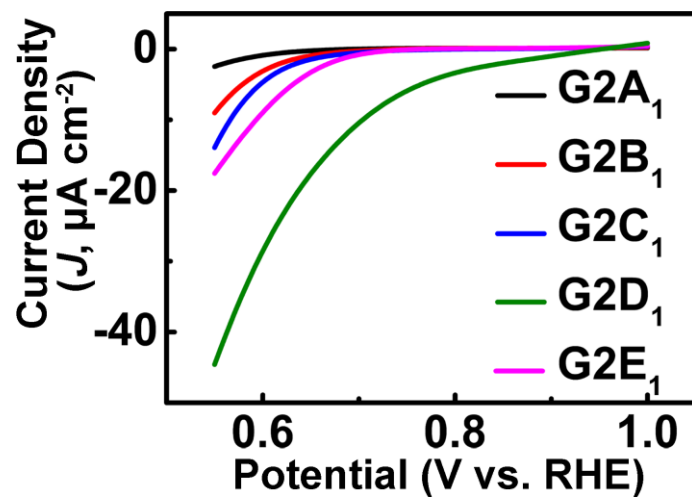
Fig. S15 ORR activity of G2 SLGs. LSVs of $G2A_1$-$G2E_1$ measured

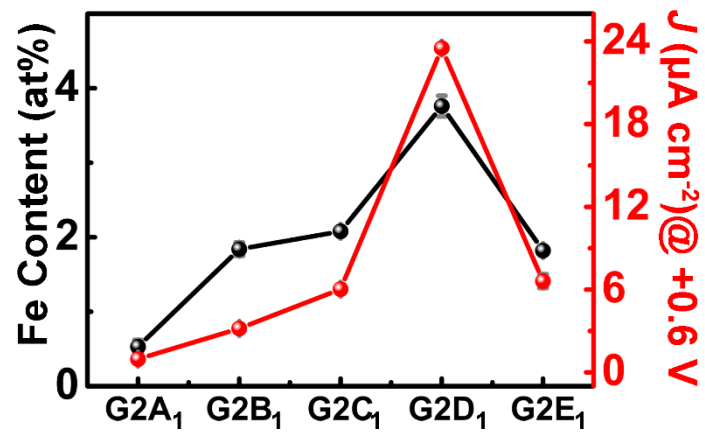in O_2-saturated 0.1 mol L^{-1} H_2SO_4 solution. (scan rate: 10 mV s^{-1})

Fig. S16 The correlation between the Fe atomic contents of $G2A_1$-$G2E_1$ and the current density at 0.6 V.
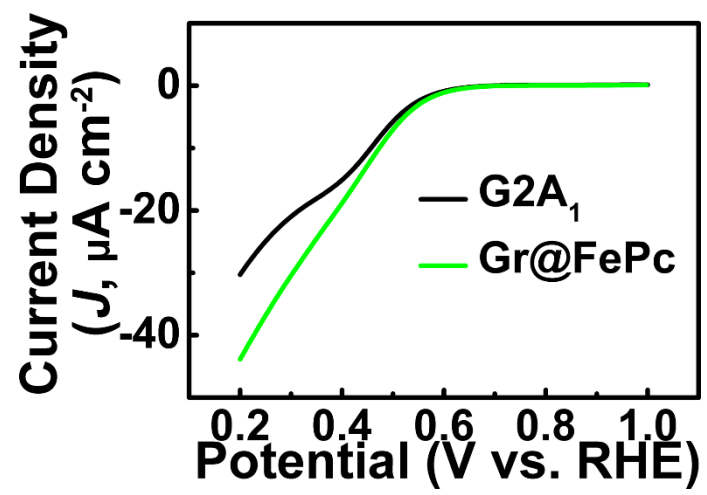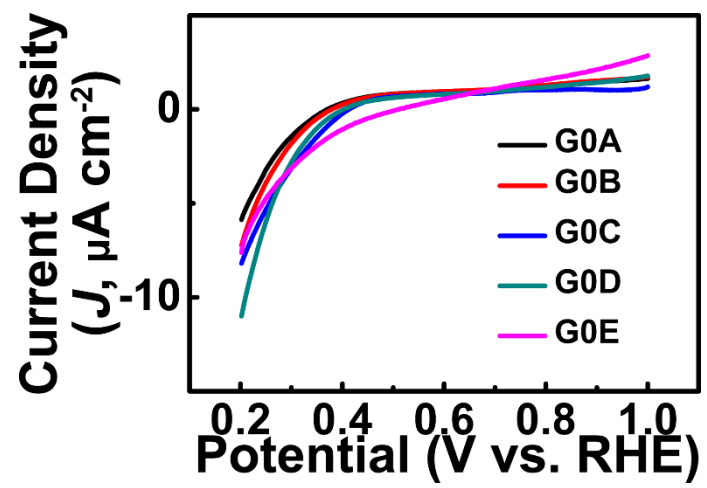
Fig. S17 LSVs of Gr@ FePc and G2A$_1$.

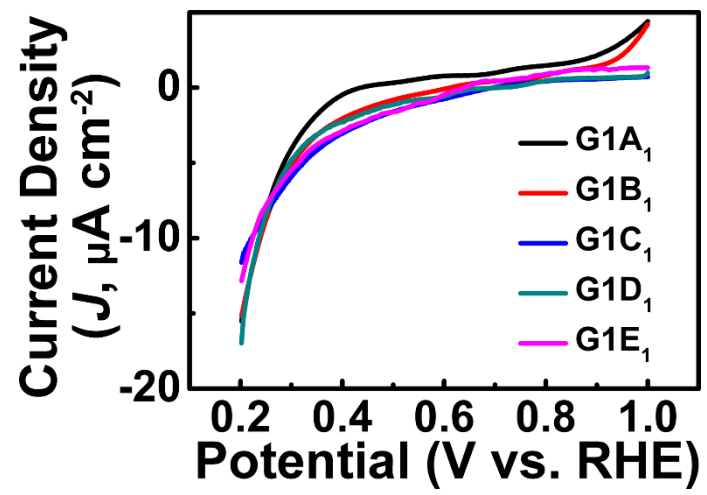**Fig. S18** LSVs of G0A-G0E.

Fig. S19 LSVs of G1A$_1$-G1E$_1$.
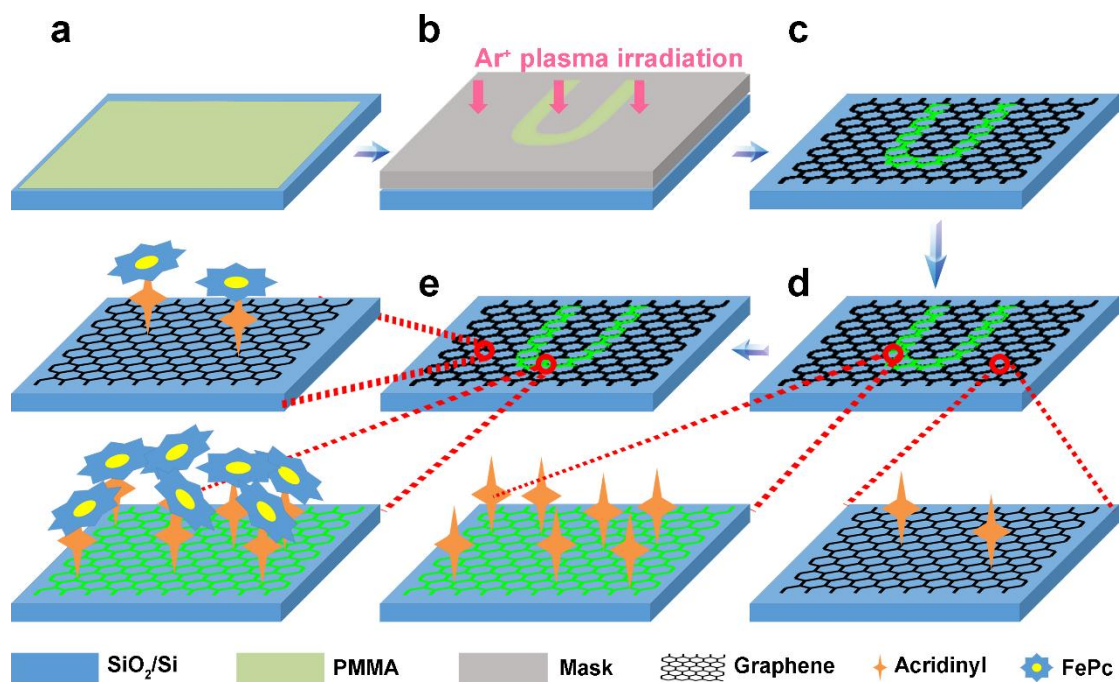
Fig. S20 Schematic diagram of the fabrication of spatial functionalization patterning on SLG.

Table S1 Summary of n_d for different SLGs.

	I_D/I_G[a]	L_d / (nm)[a]	n_d / (cm^{-2})[a]
G0A	-	100.0[b]	3.185×10^9
G0B	0.514±0.020	14.342±0.292	$(1.550\pm0.064)\times10^{11}$
G0C	1.047±0.114	9.661±0.673	$(3.453\pm0.437)\times10^{11}$
G0D	2.891±0.284	4.536±0.575	$(1.625\pm0.508)\times10^{12}$
G0E	2.075±0.257	1.957±0.154	$(8.443\pm1.260)\times10^{12}$

[a]Errors represent the standard deviation in deducing the defect density of SLGs using eight Raman spectra measured

(G0A-G0E). [b]Mean distance between defects with 100 nm was considered for defect-free pristine graphene (G0A).

Table S2 Summary of n_d, C at.%, N at.%, C_g at.% and degree of functionalization ($F_{SLG,1}$) for G1A$_1$ to G1E$_1$ and G1$_{opt,1}$.

Samp.	n_d / (cm^{-2})[a]	C 1s / (at.%)[b]	N 1s / (at.%)[b]	C_g / (at.%)	$F_{SLG,1}$ / (%)
G1A$_1$	3.185×10^9	98.80±0.10	1.20±0.10	92.79±0.72	1.30±0.11
G1B$_1$	$(1.550\pm0.064)\times10^{11}$	97.91±0.09	2.09±0.09	87.48±0.66	2.39±0.12
G1C$_1$	$(3.453\pm0.437)\times10^{11}$	97.29±0.39	2.71±0.39	78.10±0.76	3.47±0.27
G1D$_1$	$(1.625\pm0.508)\times10^{12}$	95.35±0.36	4.65±0.36	72.08±1.61	6.47±0.68
G1E$_1$	$(8.443\pm1.260)\times10^{12}$	96.54±0.56	3.46±0.56	73.01±0.75	4.74±0.51
G1$_{opt,1}$	$(2.237\pm0.520)\times10^{12}$	95.00±0.32	5.00±0.32	69.98±1.93	7.16±0.67

[a]Errors represent RSD in deducing n_d of SLGs using averaged Raman spectra. [b]Errors represent RSD of atomic content arising from three parallel batches based on XPS data.

Table S3 Summary of n_d, C at.%, N at.%, C_g at.% and $F_{SLG,2}$ for G1A$_2$ to G1E$_2$.

Samp.	n_d / (cm^{-2})[a]	C 1s / (at.%)[b]	N 1s / (at./%)[b]	C_g / (at.%)	$F_{SLG,2}$ / (%)
G1A$_2$	3.185×10^9	98.65 ±0.02	1.35 ±0.02	81.10 ±0.24	1.66 ±0.03
G1B$_2$	$(9.670 \pm 0.780) \times 10^{10}$	98.23 ±0.02	1.77 ±0.02	74.66 ±0.98	2.35 ±0.03
G1C$_2$	$(2.679 \pm 0.246) \times 10^{11}$	97.85 ±0.22	2.15 ±0.22	68.57 ±0.69	3.09 ±0.45
G1D$_2$	$(1.212 \pm 0.112) \times 10^{12}$	96.75 ±0.20	3.25 ±0.20	59.96 ±0.20	5.97 ±0.69
G1E$_2$	$(1.072 \pm 0.642) \times 10^{13}$	97.57 ±0.31	2.43 ±0.31	65.49 ±3.66	3.71 ±0.72

[a]Errors represent RSD in deducing n_d of SLGs using averaged Raman spectra. [b]Errors represent RSD of atomic content arising from three parallel batches based on XPS data.

Table S4 Summary of n_d, C at.%, N at.%, C_g at.% and $F_{SLG,3}$ for G1A$_3$ to G1E$_3$.

Samp.	n_d / (cm^{-2})^a	C 1s / (at./%)^b	N 1s / (at./%)^b	C_g / (at.%)	$F_{SLG,3}$ / (%)
G1A$_3$	3.185×10^9	94.24 ± 0.13	5.76 ± 0.13	59.71 ± 0.90	9.64 ± 0.36
G1B$_3$	$(8.848 \pm 1.101) \times 10^{10}$	93.61 ± 0.22	6.39 ± 0.22	55.30 ± 1.53	11.56 ± 0.72
G1C$_3$	$(2.907 \pm 0.215) \times 10^{11}$	92.61 ± 0.37	7.39 ± 0.37	48.30 ± 2.56	15.33 ± 1.57
G1D$_3$	$(1.064 \pm 0.186) \times 10^{12}$	91.32 ± 0.06	8.68 ± 0.06	39.28 ± 0.44	22.09 ± 0.41
G1E$_3$	$(1.019 \pm 0.030) \times 10^{13}$	93.29 ± 0.16	6.71 ± 0.16	53.06 ± 1.14	12.64 ± 0.58

[a]Errors represent RSD in deducing n_d of SLGs using averaged Raman spectra. [b]Errors represent RSD of atomic content arising from three parallel batches based on XPS data.

Table S5 Summary of different r_a, F_a, and F_p for different aryl radical additions.

Samps.	r_a / (nm)	F_a / (%)	F_p / (%)	Adj. R^2
G1A$_1$-G1E$_1$	3.2±0.1	9.5±0.3	1.30±0.11	0.9965
G1A$_2$-G1E$_2$	3.4±0.2	8.8±0.9	1.66±0.03	0.9935
G1A$_3$-G1E$_3$	3.3±0.1	32.0±0.3	9.64±0.36	0.9995

Table S6 Summary of Fe at.% and current density of linear scanning voltammogram (LSV) at 0.6 V of $G2A_1$-$G2E_1$.

Samp.	Fe 2p / (at.%)[a]	J @+600 mV / (μA cm^{-2})[b]
$G2A_1$	0.25 ±0.01	0.960 ±0.119
$G2B_1$	0.42 ±0.04	3.177 ±0.089
$G2C_1$	1.10 ±0.11	6.029 ±1.905
$G2D_1$	1.40 ±0.02	23.512 ±4.303
$G2E_1$	1.17 ±0.07	6.612 ±3.326

[a] represent RSD of atomic content arising from three parallel batches based on XPS data. [c] Errors represent RSD of current density in testing LSVs collected for samples from three parallel batches.

Supplementary Reference

1   M. M. Lucchese, F. Stavale, E. H. M. Ferreira, C. Vilani, M. V. O. Moutinho, R. B. Capaz, C. A. Achete and A. Jorio, *Carbon*, 2010, **48**, 1592.

2   L. G. Cançado, A. Jorio, E. H. M. Ferreira, F. Stavale, C. A. Achete, R. B. Capaz, M. V. O. Moutinho, A. Lombardo, T. S. Kulmala and A. C. Ferrari, *Nano Lett.*, 2011, **11**, 3190.

3   R. Cao, R. Thapa, H. Kim, X. Xu, M. G. Kim, Q. Li, N. Park, M. Liu and J. Cho, *Nat. Commun.*, 2013, **4**, 2076.

4   L. Zhang, J. Yu, M. Yang, Q. Xie, H. Peng and Z. Liu, *Nat. Commun.*, 2013, **4**, 1443.

5   A. Eckmann, A. Felten, A. Mishchenko, L. Britnell, R. Krupke, K. S. Novoselov and C. Casiraghi, *Nano Lett.*, 2012, **12**, 3925.

6   Q. Yang, W. Liu, B. Wang, W. Zhang, X. Zeng, C. Zhang, Y. Qin, X. Sun, T. Wu, J. Liu, F. Huo and J. Lu, *Nat. Commun.*, 2017, **8**, 14429.